



## Preparation of Polyaniline/Zinc Oxide Nanocomposite Thin Films by Microwave Plasma

Ahmed S. Wasfi<sup>1\*</sup>, Hammad R. Humud<sup>1</sup>, Mohammed A. Abed<sup>2</sup>,  
Mohammed E. Ismael<sup>1</sup>

<sup>1</sup>Department of Physics, College of Science, University of Baghdad, Iraq

<sup>2</sup>Department of Physics, College of Science, University of Thi-qar, Iraq

**Abstract :** Polyaniline (PANI)/ZnO nanocomposite thin films were prepared through polymerization in a microwave plasma system that was built in our laboratory. The maximum attained plasma electron temperature and density were 0.5 eV and  $1.75 \times 10^{17} \text{ cm}^{-3}$ , respectively. ZnO powder of 50 nm average particle size was used to prepare the PANI/ZnO nanocomposite thin films. They were characterized by UV-VIS, FTIR, AFM and SEM to study the influence of zinc oxide nanoparticles on the optical properties, morphology and structure of the thin films. The optical properties studies indicated that the optical energy band gap of the PANI/ZnO nanocomposite decreased systematically from 3.50 eV to 3.37 eV with increasing ZnO nanoparticles concentration from 1 to 9 wt% respectively. FTIR measurement revealed a shift in the FTIR absorption peaks with ZnO concentration. AFM and SEM images indicated a uniform distribution of the ZnO nanoparticles in the PANI matrix. It can be concluded that PANI/ZnO nanocomposite thin films of good morphological quality and controlled optical energy band gap, which could be suitable for the supercapacitor applications, can be prepared by microwave plasma polymerization technique.

**Keywords :** plasma polymerization, polyaniline nanocomposite, microwave induced plasma.

### Introduction:

In recent years, improvement of polymer/inorganic hybrid materials on the nanometer scale has been receiving important attention due to their wide range of possible applications in optoelectronic devices [1, 2]. ZnO is one of the typical n-type semiconductors, while polyaniline, as is one of the typical conductive polymers, is usually considered as p-type material [3, 4]. Inorganic nanoparticles such as ZnO have so far been encapsulated into the shell of conducting polymers giving rise to a host of dissimilar nanocomposites[1]. The nanocomposites of metal and semiconductor particles are important in several optical and electronic applications. Nano scale particles are more attractive due to their remarkable properties arising from the nanosize and large surface area. The insertion of nanoscale fillers may improve the electrical and sensing properties of polymers [5-7]. Polyaniline (PANI) is one of the promising conducting polymers due to its high conductivity, simplicity of preparation, and good environmental stability, which makes it appropriate as a matrix for preparation of conducting polymer

nanocomposites[8, 9]. Polymers are usually polyconjugated structures which are insulators in their pure state; but when treated with oxidizing or reducing agents they can be converted into compounds having reasonable electrical conductivity [10].

In a polymer, the  $\pi$  electrons are not tightly bound and they become delocalized along the polymer chain. In 1950, Rudolf Peierls found that it is energetically favorable for polymer chains to be distorted spontaneously, creating a gap between the filled valence and the unfilled conduction band converting a chain from a conductor to a semiconductor [10].

In the present work, nanocomposite thin films of polyaniline with zinc oxide nanoparticles were deposited on glass substrates by microwave plasma polymerization of aniline. Optical properties, morphology and structure of these thin films were investigated.

### Experimental set-up:

Our home-built microwave induced plasma (MIP) system consisted of cylindrical stainless steel vacuum chamber of 10 cm inner diameter and 30 cm length. The cylindrical chamber has many ports, one of which is coupled to a double stage rotary vane vacuum pump of  $8\text{ m}^3/\text{hp}$  pumping speed from Leybold Heraeus Co., to maintain a vacuum of about  $10^{-3}$  mbar in the chamber. The other port is used to introduce the sample (aniline with ZnO nanoparticles) which can be injected to the plasma chamber using a car electrical fuel injector nozzle that is working as an electrical vacuum valve to introduce a pressurized liquid mixture to the vacuum chamber as a spray pulse of very tiny drops that immediately vaporized in the vacuum. The quantity of the injected spray can be controlled by a special electrical circuit designed to control the spray pulse duration. Furthermore, there is a borosilicate glass view window fixed at the side port which is used to monitor the plasma spectrum of the reacting species by an optical spectrometer. The viewport is employed also as a quick access door which can be used to feed the samples into the plasma reaction chamber. The two axial end ports of the cylindrical chamber are closed with two flanges that have circular holes at their centers where a quartz glass tube is passed through along the cylindrical chamber axis. The inside of the tube was at atmospheric pressure whereas the outside was at low pressure. After proper evacuation time, Argon was fed to the chamber, as a working plasma gas, through a needle valve that controls the gas flow precisely. The filling pressure in the chamber was monitored using a Pirani gauge. To avoid the heating due to the plasma in the chamber, an air blower was fixed at one end of the quartz tube.

Microwave was generated by means of 750 watt magnetron, working at a frequency of 2.45 GHz, and was transmitted to the plasma chamber through a rectangular waveguide which holds a  $\text{TE}_{10}$  transmission mode. A copper pipe of 6 mm diameter was inserted at the other end of the glass tube through the waveguide at a certain position that represents a maximum of the standing wave oscillating in it. This copper pipe acts as an antenna that conducts the microwave radiation from the waveguide to the vacuum chamber. A cylindrical plasma column was obtained around the quartz tube inside the chamber as a result of the propagation of electromagnetic surface wave plasma (SWP). In fact, this configuration can be considered as a coaxial cable transmission line where the copper pipe represents the central conductor of the cable, the glass tube its outer insulator and the generated plasma, which is a conductive medium, replaces the missing outer conductor of the coaxial cable. When the electric field strength, which is transmitted through the copper antenna, exceeds the breakdown field strength of argon gas, discharge ignites at the low pressure regime inside the chamber. Increasing the microwave power, the axially homogeneous plasma grows along the quartz tube. The space occupied by the plasma is proportional to many factors such as the microwave power and working gas pressure.

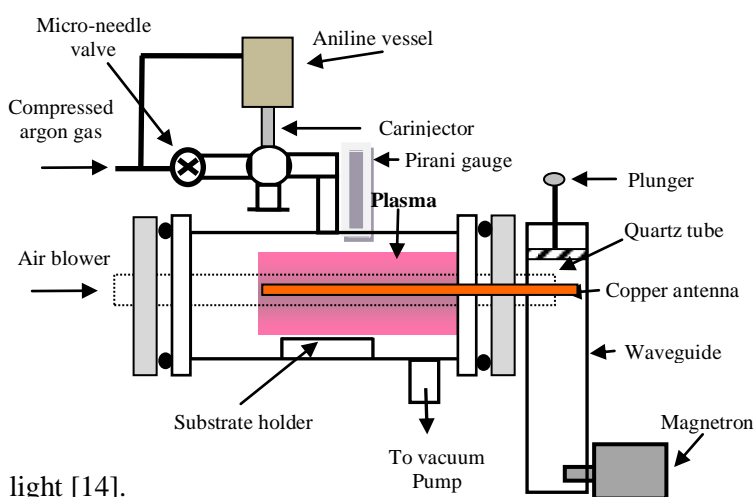
The diagnostic of the microwave argon plasma was done in an earlier work [11], in order to optimize our system and ensure that the MIP system is capable of producing reproducible films of good quality. Optical emission spectroscopy was used as a plasma diagnostic method; it gives very interesting information on the plasma parameters such as plasma electron temperature and density, and on the influence of the process parameters such as microwave power and working gas pressure. The electron temperature was determined using the ratio of two argon plasma spectral lines' intensity method [12,13]. The maximum attainable plasma electron temperature and density were 0.5 eV and  $1.75 \times 10^{17} \text{ cm}^{-3}$ , respectively.

After a proper cleaning procedure, the glass substrate was fixed just below the plasma to avoid burning the deposited polymer films within the plasma. Different concentrations (1, 5, 9 wt.%) of ZnO mixed with aniline were used to deposit PANI/ZnO nanocomposite thin films on glass substrates. The thickness of the deposited films depends on the quantity of the mixture injected in the Ar plasma as a spray pulse of controlled duration. This control of the spray pulse duration and their repetition with time were necessary to keep the working pressure in the chamber within the 0.5-1.0 mbar range, which is of great importance to maintain the plasma working. A schematic diagram and a photograph of the experimental arrangement are shown in Figure 1.

The film thickness ( $t$ ) was measured using the optical interference method employing 532 nm laser beam. It was determined using the equation:

$$t = (\lambda/2)(x/\Delta x) \quad \dots\dots\dots (1)$$

where  $\Delta x$  is the width of the interference fringe,  $x$  is the position of the fringes, and  $\lambda$  is the wavelength of the used



light [14].

**Figure1: schematic diagram and a photograph of the experimental arrangement.**

## Results and discussion:

FTIR spectra of thin films of pure PANI and PANI/ZnO nanocomposite with 5 wt.%ZnO, Figure 2, were taken to estimate the interactions among PANI and ZnO nanoparticles. These spectra were recorded using solid KBr discs and all samples were tested using a Shimadzu Co. FTIR 8000 series instrument in the 400-4000  $\text{cm}^{-1}$  wavelength range.

The characteristic peaks of pure PANI at 1575  $\text{cm}^{-1}$  and 1456  $\text{cm}^{-1}$  are due to the presence of quinoid and benzenoid rings, respectively, and they can be assigned to the C=C ring asymmetric and symmetric stretching vibrations. The peak at 2927  $\text{cm}^{-1}$  corresponds to C-H stretching of aromatic ring, and the peak at 3429  $\text{cm}^{-1}$  can be attributed to the N-H stretching. The peak at 1334  $\text{cm}^{-1}$  represents the C-N stretching of primary aromatic amines, while the peak at 1161  $\text{cm}^{-1}$  corresponds to the C-H bending vibration [6].

The PANI/ZnO composite spectrum also shows the same characteristic peaks. However, as compared to those of pure PANI the corresponding peaks of PANI/ZnO composite are shifted from 1575  $\text{cm}^{-1}$  to 1550  $\text{cm}^{-1}$ , 2927  $\text{cm}^{-1}$  to 2867  $\text{cm}^{-1}$ , 3429  $\text{cm}^{-1}$  to 3440  $\text{cm}^{-1}$  and 1334  $\text{cm}^{-1}$  to 1340  $\text{cm}^{-1}$ . These shifts may be attributed to the formation of hydrogen bonds between ZnO and NH group of PANI on the surface of ZnO nanoparticles.

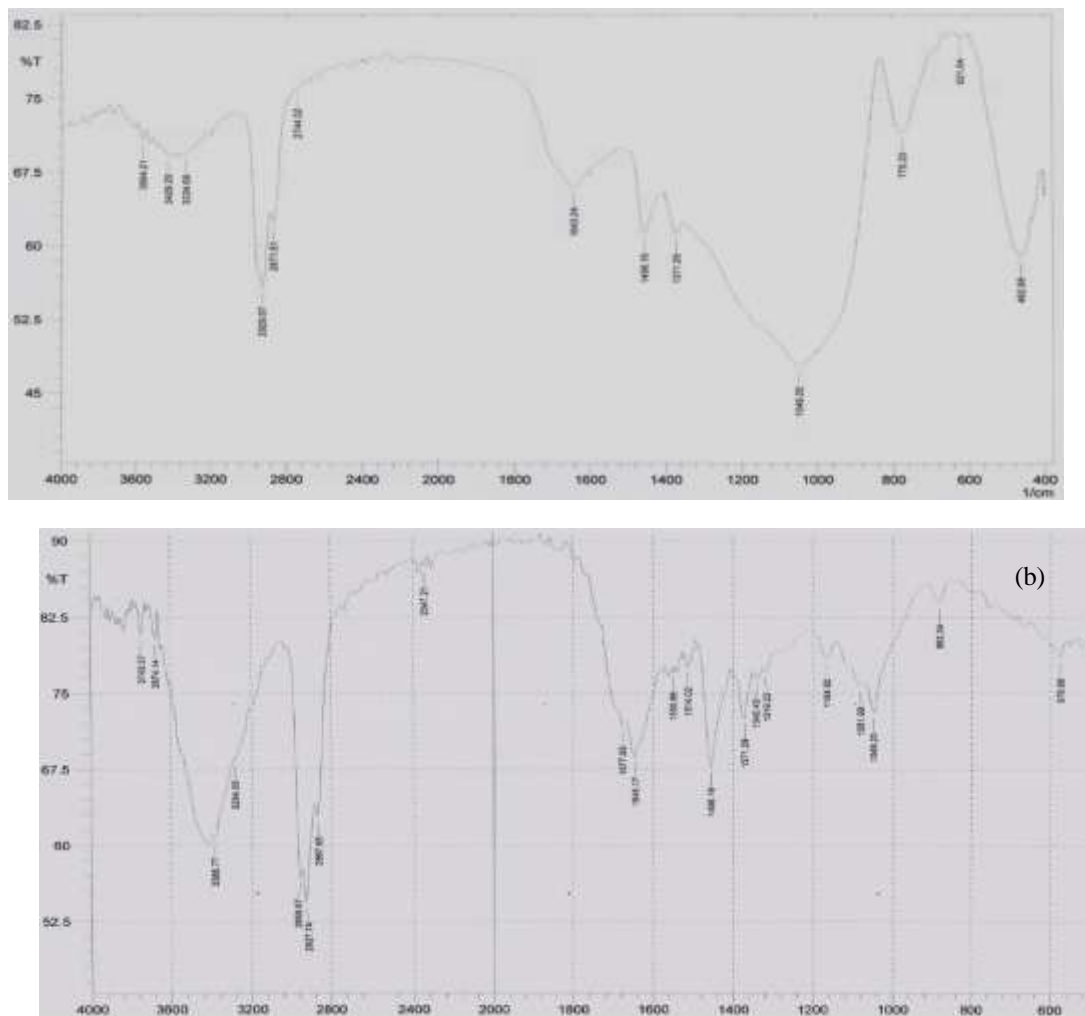


Figure 2:FTIR spectra of (a) pure PANI and (b) PANI/ZnO nanocomposite of 5wt.% ZnO thin films.

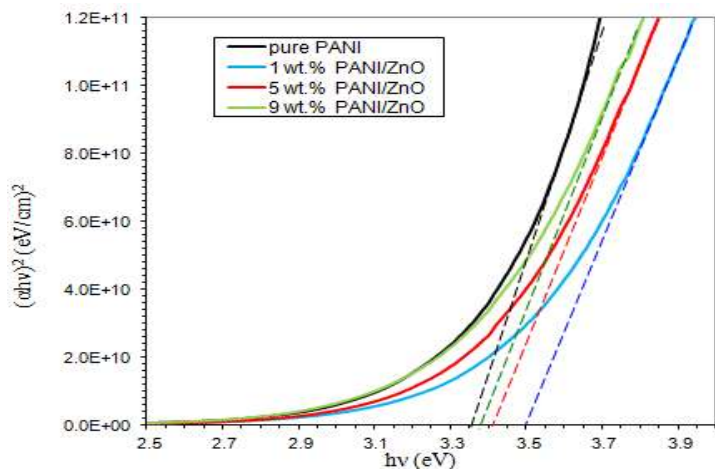


Figure 3:variation of  $(\alpha hv)^2$  with photon energy ( $h\nu$ ) of pure PANI and PANI/ZnO nanocomposite thin films using different ZnO concentrations.

The variation of  $(\alpha h\nu)^2$  with  $(h\nu)$  is shown in Figure 3, where  $\alpha$  is the absorption coefficient obtained from the absorption spectrum measurements of the deposited films and  $(h\nu)$  is the incident photon energy, for PANI/ZnO nanocomposite thin films deposited at the same distance (3.4 cm) from the plasma axis and for the same deposition time with different ZnO concentrations (pure PANI, 1, 5, and 9 wt.% ZnO). The curves have straight portions, which imply that the samples undergo direct transition. The optical energy band gaps were extracted by extrapolating the straight portions of the graphs on the  $(h\nu)$  axis at  $\alpha = 0$  [6]. The corresponding results are listed in Table 1.

**Table 1: thickness (nm), optical energy gap ( $E_g$ ) of pure PANI and PANI/ZnO of different ZnO weight concentrations thin films.**

ZnO concentration wt%	Film thickness (nm)	$E_g$ (eV)
Pure PANI	165	3.35
1	177	3.50
5	190	3.41
9	194	3.37

The addition of 1 wt.% of ZnO to PANI increased the optical energy gap from 3.35 eV that of pure PANI film to 3.50 eV. This may be due to the improvement in the polymer structural stability. A fact that was clear in the good reproducibility of the results. At the same time, increasing the zinc oxide weight percentage in the nanocomposite thin films toward 9 wt.% leads to a decrease in the optical energy gap from 3.50 to 3.37 eV. This reduction in the optical energy gap is most probably due to the effective disordering of the polymer structure that results in an increase in the localized energy state within the optical energy gap.

The morphological characteristics of PANI/ZnO nanocomposite thin films were studied by atomic force microscopy (AFM) to monitor the structural changes due to the addition of ZnO nanoparticles of 9 wt.% concentration, and to compare them with the structure of a pure polyaniline thin film. Two and three-dimensional AFM images of PANI/ZnO thin film of 9 wt.% ZnO are shown in Figure 4. It is found that the surface roughness average of the pure polyaniline thin film is 2.45 nm and the average particle diameter is 100.78 nm, while those for PANI/ZnO thin film are 2.31 nm and 94.27 nm, respectively.

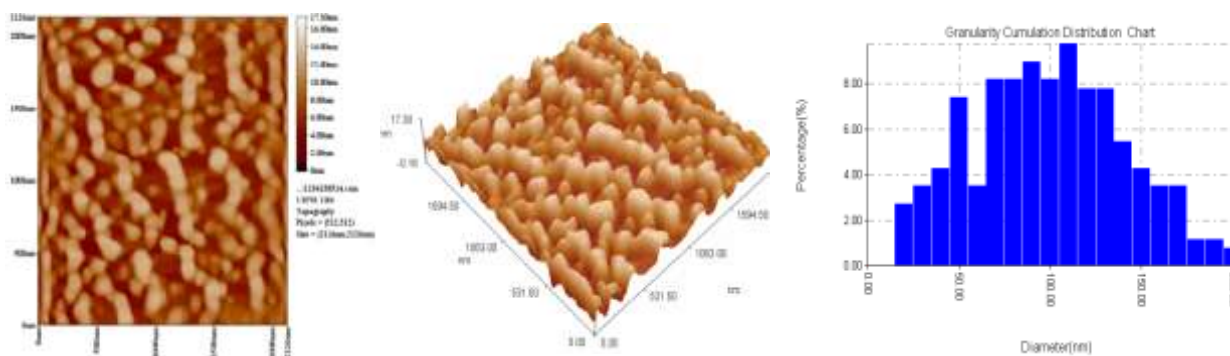


**Figure 4: AFM photographs of 9 wt.% ZnO PANI/ZnO thin film of: 2D image, 3D image and cumulative granularity distribution chart.**

SEM images of PANI/ZnO nanocomposite thin films of 1 wt.% and 9 wt.% ZnO concentrations are shown in Figure 5. As it can be seen, the ZnO nanoparticles are attached to the polyaniline chains during polymerization. The images indicate that there is a uniform distribution of the ZnO nanoparticles, which are spherical in shape, in the PANI matrix with few ZnO clusters.

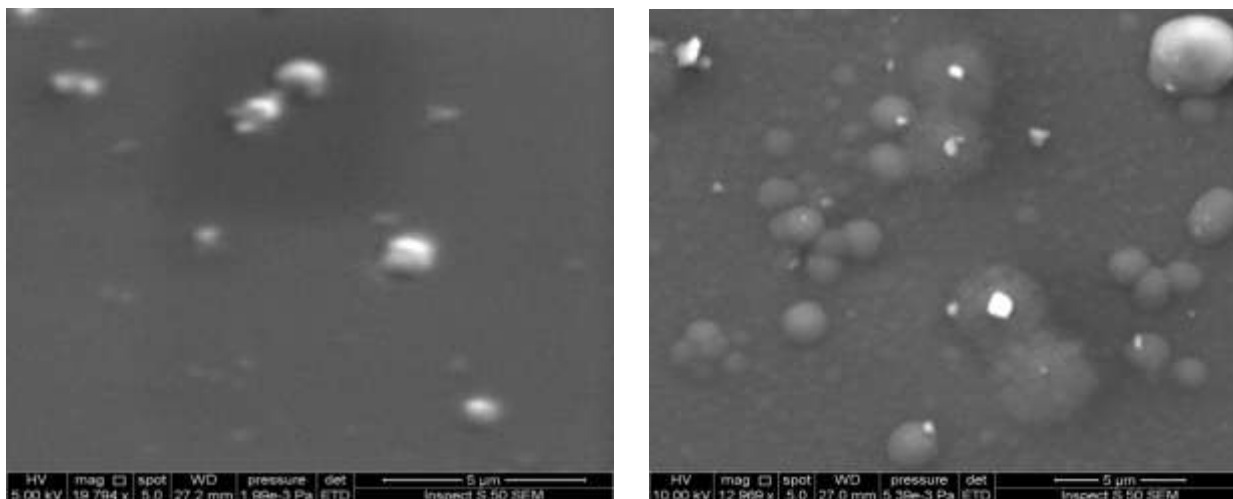


**Figure 5: SEM images of PANI/ZnO nanocomposite thin films of 1wt.% and 9 wt.% ZnO concentrations.**

### Conclusion:

Polymerization by microwave plasma technique can be employed to produce extremely smooth polyaniline/metal oxide nanocomposite thin films with small surface roughness as compared with films prepared by other techniques. The nanoparticles are uniformly distributed in the polyaniline matrix. Addition of ZnO nanoparticles in small concentration percentage increased the optical energy band gap of pure PANI to some extent and then decreased with increasing their concentration percentage. This may be due to the interaction between ZnO nanoparticles and PANI, in addition to the polymer structural changes.

### Acknowledgment:

We are thankful to Prof. Raad M.S. Al Haddad for very helpful discussions, Dr. Zainab Al Shaibani for language proofreading and Eng. Mazen Al Ansari for his technical help.

### References:

1. C. L. Zhu, S.W. Chou, S. F. He, W. N. Liao, and C. Chen, "Synthesis of core/shell metal oxide/polyaniline nanocomposites and hollow polyaniline capsules," *Nanotechnology*, Vol. 18, No. 27, ID 275604, 2007, 6 pages.
2. S. Srivastava, S. Kumar, V. N. Singh, M. Singh, and Y. K. Vijay, "Synthesis and characterization of TiO<sub>2</sub> doped polyaniline composites for hydrogen gas sensing," *International Journal of Hydrogen Energy*, Vol. 36, No. 10, 2011, pp. 6343–6355.
3. L.-C. Ji, L. Huang, Y. Liu et al., "Optical and electrical properties of zinc oxide/indium/zinc oxide multilayer structures," *Thin Solid Films*, Vol. 519, No. 11, 2011, pp. 3789–3791.
4. M. Mekewi, A. Shebi, A. I. Iman, M. S. Amin, and T. Albert, "Screening the insecticidal efficacy of nanoZnO synthesized via in-situ polymerization of crosslinked polyacrylic acid as a template," *Journal of Materials Science & Technology*, Vol. 28, No.11, 2012, pp. 961–968.
5. L. Geng, Y. Zhao, X. Huang, S. Wang, S. Zhang, and S. Wu, "Characterization and gas sensitivity study of polyaniline/SnO<sub>2</sub> hybrid material prepared by hydrothermal route," *Sensors and Actuators B*, Vol. 120, No. 2, 2007, pp. 568–572.
6. K. Gupta, P. C. Jana and A. K. Meikap, "Optical and Electrical Transport Properties of Polyaniline-Silver Nanocomposite," *Synthetic Metals*, Vol. 160, No. 13-14, 2010, pp. 1566-1573.

7. A. Choudhury, "Polyaniline/Silver Nanocomposites: Di-electric Properties and Ethanol Vapour Sensitivity," *Sensors and Actuators B: Chemical*, Vol. 138, No. 1, 2009, pp. 318-325.
8. Y. Dong, Y. Ma, T. Zhai, Y. Zeng, H. Fu, and J. Yao, "A novel approach to the construction of core-shell gold-polyaniline nanoparticles," *Nanotechnology*, Vol. 18, No. 45, Article ID 455603, 2007, 6 pages.
9. A. R. B. M. Yusoff and S. A. Shuib, "Metal-base transistor based on simple polyaniline electropolymerization," *Electrochimica Acta*, Vol. 58, No. 1, 2011, pp. 417-421.
10. G. B. Shumaila, V. S. Lakshmi, M. Alam, A. M. Siddiqui, M. Zulfequar and M. Husain, "Synthesis and Characterization of Se Doped Polyaniline," *Current Applied Physics*, Vol. 11, No. 2, 2010, pp. 217-222.
11. A. S. Wasfi, H. R. Humud, M. E. Ismail, "Spectroscopic measurements of the electron temperature in low pressure microwave (2.45GHz) argon plasma", *Iraqi Journal of Physics*, Vol.13, No.27, 2015, pp. 1-12.
12. A. Ancona, T. Sibillano, P.M. Lugará, "Optical plasma spectroscopy as a tool for monitoring laser welding processes," *Journal of Achievements in Materials and Manufacturing Engineering*, Vol. 31, Issue 2, 2008, pp. 402-407.
13. A. Palmero, E. D. van Hattum, H. Rudolph, and F. H. P. M. Habraken, "Characterization of a low-pressure argon plasma using optical emission spectroscopy and a global model," *Journal of Applied Physics*, Vol. 101, 2007, 053306.
14. L. Eckortova, "Physics of Thin Films", Plenum press, New York and London, (1977).

\*\*\*\*\*